2020 IMEKO TC-4 International Conference on
Metrology for Archaeology and Cultural Heritage
Trento, Italy, October 22-24, 2020

Thermal decay of monzogranite from Elba Island (western Tuscany, Italy): properties of an ancient building material

Andrea Aquino[1], Michele Antola[1], Alessio Pacchini[1], Stefano Pagnotta[2], Marco Lezzerini[1]

[1] *Department of Earth Sciences, University of Pisa, Via Santa Maria 53 – 56126 Pisa, Italy*
andrea.aquino@phd.unipi.it, marco.lezzerini@unipi.it
[2] *Chemistry and Industrial Chemistry Department, University of Pisa, Via G. Moruzzi 13 – 56124 Pisa, Italy stefanopagnotta@yahoo.it*

Abstract **– Thermal decay may be one of the causes of monzogranite deterioration. In this work, we study the chemical, mineralogical and petrographic characteristics and the physical properties of the monzogranite of Elba Island as a building material, to better understand the main effects of the degradation caused by artificial thermal cycles on this rock.**

I. INTRODUCTION

As part of the research aimed at studying the physical and mechanical characteristics of the stones used in the monumental building of the city of Pisa [1-8], we focus this work on the monzogranite of Mt. Capanne (Elba Island). This stone material, well known from a chemical, mineralogical and petrographic point of view, has been cultivated since Roman times and even in the city of Pisa, we can observe its wide use as a building material, for example, in some columns of the leaning Tower, in some parts of the paving of a Borgo Stretto, in the curbs of the sidewalks.

The main purpose of this work is to identify and assess the effects of degradation on this rock produced by thermal oscillations.

To achieve this goal, we needed to fine-tune some methodologies for measuring the physical properties of the studied material. The monzogranite sampling took place in some active quarries in the south-eastern area of Elba island. The samples collected were characterized from a chemical, mineralogical, petrographic, and physical point of view. The analyses of the physical properties were repeated on the same samples after subjecting them to heat treatments. The obtained dataset was used to attempt an interpretation of the relationships between the various characteristics of the studied samples and the thermal degradation.

II. GEOLOGICAL SETTING

The Elba Island, located in front of the southern Tuscan coast in the Northern Tyrrhenian Sea, relates to the so called Tuscan Magmatic Province. During the late Miocene-Pleistocene an intense magmatic activity, related to the post-collisional phase of the Apennine orogeny, took place along the Tyrrhenian border of the Italian Peninsula [9-11] emplacing a wide variety of rock, from intrusive to volcanic, from strongly alkaline to calc-alkaline [12-17].

There are mainly two different monzogranitic plutonic masses outcropping both in the west and east of Elba Island: Monte Capanne, 6.9 Ma and La Serra-Porto Azzurro, 5.9 Ma, respectively, along with their microgranite, aplite and pegmatite dyke swarms [18–25].

The monzogranitic Monte Capanne pluton [26–31] is fed by different magma pulses that then coalesced into one single intrusion [32]. It is possible to distinguish three main facies in the pluton where the first two are the most important: 1) the monzogranitic Sant'Andrea facies, characterized by numerous large K-feldspar megacrysts and mafic enclaves; 2) the granodioritic-monzogranitic San Piero facies, typically quarried for its homogeneous texture almost devoid of large megacrysts and mafic enclaves, and therefore studied for the purposes of this work; 3) San Francesco facies show intermediate features between the 1) and 2) facies [26, 31].

The study of the thermal degradation of a rock is fundamental to understand the durability of the rock itself and it becomes of extreme importance for the building materials. Temperature variations can generate tensions inside the rock developed due to the different thermal behaviour of the minerals. For this reason, when a granular disintegration process occurs it can lead to the transformation of the material into an incoherent mass of granules. The granular disintegration is one of the most relevant phenomena that cause the disruption of monzogranite building and ornamental works. In this work we try to evaluate whether thermal oscillation can be one of the causes of the disintegration of the monzogranite itself.

III. USES OF MONZOGRANITE FROM ELBA ISLAND AS A BUILDING MATERIAL

The exploitation of the monzogranite from Elba Island traces back to Roman times (Pantheon) and it is still possible to see traces of the ancient cultivation methods used on the island of Elba [33]. Some ancient abandoned quarries near the village of Cavoli show the excavation technique practiced in Roman: in particular, in a small quarry front we can still observe the holes where wooden wedges were forced in, then repeatedly wet until the wood, swelling, cracked the rock apart. Numerous remains of Roman monzogranite columns, currently covered by thick vegetation, were found in the areas surrounding the village of Cavoli. There are other artifacts, found on the island, attesting extraction and processing of the monzogranite during Roman times like the altar of Attiano, found near Seccheto and the so-called "ship", a semi-finished product with two protrusions along a stone cylinder recalling the prow of a ship. The exploitation process of the monzogranite resumes during the Pisan domination of the island in the Middle Ages; this is witnessed by the appearance of this stone material in some medieval buildings in Pisa, mainly for producing columns used in the interior of the buildings, rarely as external ones [34]: mainly re-used material (for example some columns of the portico of San Zeno, of the Pieve di Calci, etc.), but there are also news related to medieval works, for example, some columns of the Cathedral of Pisa, of the Church of San Paolo a Ripa d'Arno and also of some columns, or parts of them, of the Leaning Tower. This stone material is currently used in Pisa, and other major cities, as a building material (for example small parts of the paving of Borgo Stretto, some portions of the coverage of the banks of the *Lungarno*, curbs of the sidewalk).

There are numerous monzogranite quarries on Monte Capanne, especially on the south western side of the pluton, most of which, unfortunately, are inactive due to the lack of manpower. There are only three active quarries today, two are in San Piero area, and one in Seccheto. The exploited material is used both for ordinary constructions (windowsills, stairways, enclosure walls, curbs of the sidewalk) and city paving and for ornamental purposes. Over the past few years, some of these quarries had troubles due to price competition of granite from China, sold at significantly lower prices.

IV. ANALITHICAL METHODS

We collected five different samples of granite from Monte Capanne pluton, on Elba Island, come from three different quarries, two in S. Piero area and one in Seccheto area. The five samples were analysed using the analytical techniques as listed below:

- chemical analysis through X-ray fluorescence [35] for the determination of major and minor compounds (Na_2O, MgO, Al_2O_3, SiO_2, P_2O_5, K_2O, CaO, TiO_2, MnO, Fe_2O_3). The measurement uncertainty results between 4-7% by weight for concentrations <1%, between 2-4% for concentrations between 1 and 10% and around 1% for concentrations > 10% [36-37].
- mineralogical analysis through X-ray diffractometry (XRD) $\lambda = 1.5406$ Å, angle range 4-66°2θ;
- petrographic analyses: transmitted light microscopic observation of thin sections (Zeiss Axioplan microscope);

physical properties of the stones like real (ρ_r) and apparent (ρ_a) density, water absorption coefficient by capillarity, water absorption at atmospheric pressure, total and open porosity and saturation index have been determined following EN standards [38-40];

- real density (ρ_r) has been determined using a gas pycnometer (ultrapycnometer 1000 by Quantachrome Corporation) [38]. The measurements were performed on approximately 10 g of very-fine- grained powders dried at 105 ± 5 °C for 24 h under the following experimental conditions: ultrahigh purity compressed Helium with outlet pressure of 140 kPa; target pressure, 100 kPa; equilibrium time, automatic; purge mode, 3 minutes of continuous flow; maximum number of runs, 6; number of averaged runs, the last three;
- apparent density (ρ_a) has been determined by ratio between dry mass and volume of each sample. The specimens were placed in a stove at 60° C until the dry weight was reached, (i.e. when the difference between two successive weighing at an interval of 24 h is not greater than 0.1 % of the mass of the specimen). Then the specimens were immersed in distilled water following [38]. The volume of the specimens was measured by means of a hydrostatic balance on water-saturated samples [41];
- water absorption coefficient by capillarity has been determined on the same samples used for apparent density determination following [39]. Measurements were taken after 1, 3, 5, 15, 30, 60, 120, 180, 240, 300, 360, 420, 480, 1440, 2880 minutes;
- the total porosity has been calculated according to (1)

$$P\ (\text{vol. }\%) = 100 \cdot (1 - \rho_a / \rho_r) \qquad (1)$$

- thermal degradation. Four different thermal degradation tests using 15 cylindric samples. Before performing the thermal degradation, each specimen was brought to constant weight and subjected to a water absorption cycle both by capillarity and by total immersion for at least 14 days. After the sample preparation the following tests were carried out: a – heating at 110 °C use 12 specimens, three for each of the 4 samples, with the help of a stove; b - heating at 150 °C using the same specimens used for the 110 °C test, with the aid of a muffle; c - heating at 350 °C using the same specimens for the 150 °C, with the help of a muffle; a heating at 150 °C using three cylindrical specimens of the same sample, with the help of a stove.

The goal of this last heating was to degrade only one base of the specimen, taking care to always rest the same base on the plate of the stove: to avoid degrading the specimen homogeneously over the entire volume, the carrot was removed from the stove when the base not resting on the plate began to heat up. At this point it was left to cool to room temperature and degraded again, all for 50 cycles. At the end of each of the four different types of degradation, all 15 specimens were again subjected to a water absorption cycle trying to evaluate whether the degradation somehow determined the alteration of the samples under study.

V. RESULTS AND DISCUSSION

The main mineralogical phases identified by XRPD analysis are feldspars, quartz and then biotite and chlorite. According to the XRD data and the petrographic study, the chemical analysis by means of XRF are reported in Table 1. As can be seen, the four samples have a SiO_2 content between 65.89% and 68.23%, an Al_2O_3 content between 15.85% and 16.16% and a K_2O content between 3.90% and 4,43%. As for the other components, their content is less than 4% and their sum is less than 13%; the sum of MnO, TiO_2 and P_2O_5 does not exceed 1%.

The petrographic analysis of twelve thin sections showed that the material under examination represents a homogeneous, holocrystalline, hypidiomorphic rock, made up of disequigranular minerals, with medium grain. By far the most abundant mineral is plagioclase, characterized by direct or oscillatory zoning with, in general, the core enriched in anorthite. The most frequent twinning is albite, the albite-Carlsbad is rare. Plagioclase sometimes includes small biotite crystals and has some secondary sericite flakes. Compared to quartz, in addition to having a slightly higher refractive index, plagioclase has a greater degree of idiomorphism. The other main minerals present are quartz, K-feldspar and biotite. The values of the modal analysis of the rock, compared with the literature data, are shown in Table 2. From the table it appears that the percentage of plagioclase is variable from 36 to 39%, the percentage of quartz varies from 28 to 30%, while the K-feldspar varies from 17 to 20% and the percentage of phyllosilicates and secondary minerals from 14 to 15%.

Following the IUGS diagram for the classification of plutonic rocks, the analysed samples can properly be defined as monzogranite.

In table 3 ed the physical properties for the analysed samples are report. The real density, ρ_r, ranges between 2.6 and 2.7 g/cm^3, while the values of the apparent density, ρ_a, are close to the former one, confirming the low porosity of the monzogranite, also according to the low values of imbibition coefficients.

*Table 1: Chemical composition of five monzogranite samples coming from Elba Island determined by XRF analysis: the major elements are expressed in oxides wt.%. *, data from literature; M., mean; st. D., standard deviation. L.O.I.: loss on ignition. Fe_2O_3: total iron expressed as Fe_2O_3.*

	L.O.I.	Na_2O	MgO	Al_2O_3	SiO_2	K_2O	CaO	Fe_2O_3	<1%
G2	0,77	2,75	2,86	15,90	65,89	4,37	2,77	3,77	0,92
AA	0,60	2,72	2,45	15,91	67,97	3,90	2,52	3,16	0,77
AB	0,47	2,58	2,81	15,95	66,83	4,43	2,63	3,44	0,86
BA	0,41	2,57	2,61	15,85	67,72	4,37	2,49	3,19	0,80
CA	0,42	2,70	2,29	16,16	68,23	4,26	2,31	2,92	0,71
*	0,54	3,23	1,51	15,91	66,98	4,11	3,17	3,78	0,77
M.	0,53	2,66	2,60	15,95	67,33	4,27	2,54	3,30	0,81
st. D.	0,14	0,07	0,21	0,11	0,86	0,19	0,15	0,29	0,07

*Table 2: Modal analysis of five monzogranite samples coming from Elba Island after petrographic analysis, wt.%. *, data from literature [42]; M., mean; st. D., standard deviation.*

	Quartz	Plagioclase	Feldspars	Phyl. + acc.
G2	28	38	19	14
AA	30	39	17	14
AB	29	36	20	15
BA	30	36	19	15
CA	30	38	18	14
*	26,9	39,5	18,3	15,3
M.	29,4	37,4	18,6	14,4
st. D.	0,80	1,20	1,02	0,49

*Table 3: Physical properties of monzogranite samples: ρ_r real density; ρ_a apparent density; P, porosity; Ci_p weight related imbibition; Ci_v volume related imbibition; S.I. saturation index; * data from literature: [1][43], [2][44].*

sample	G2	AA	AB	BA	CA	*
ρ_r (g/cm^3)	2,696 ±0,003	2,698 ±0,002	2,696 ±0,002	2,696 ±0,002	2,687 ±0,002	2,6-2,7[1]
ρ_a (g/cm^3)	2,650 ±0,002	2,647 ±0,003	2,647 ±0,003	2,651 ±0,008	2,630 ±0,003	2,63 [2]
P (%)	1,72 ±0,08	1,890 ±0,152	1,816 ±0,178	1,661 ±0,289	2,121 ±0,104	0,5-1,5[1]
W.A.C.	0,217 ±0,010	0,186 ±0,10	0,212 ±0,30	0,215 ±0,20	0,238 ±0,30	-
Ci_p (%)	0,43 ±0,01	0,40 ±0,01	0,40 ±0,01	0,41 ±0,01	0,45 ±0,01	-
Ci_v (%)	1,13 ±0,03	1,06 ±0,03	1,06 ±0,03	1,09 ±0,04	1,18 ±0,02	-
S.I. (%)	66 ±4	56 ±2	58 ±3	65 ±9	56 ±6	-

We used water absorption by capillarity as method to relate the variations of the water absorption speed compared to different degradation states. Figures 1-4 show the different curves for water absorption by capillarity of the analysed samples with different degradations. During the first 24 hours the curves show a steeper slope, while after a day they are less steep, asymptotically aiming to a constant value. This means that over time the absorption rate slows down, and the filling of the residual porosity becomes slower. The dotted lines in the graphs represent the verso surface of the specimens. The water absorption curves by capillarity for heating at 60 °C and 110 °C do not show great differences, while the curves relating to the samples heated up to 150 °C show a greater increase in absorption. Samples degraded at 350 °C show the highest rate of water absorption. In addition, as can be seen, in each graph the verso surface has a lower water absorption rate than the average of the other surfaces.

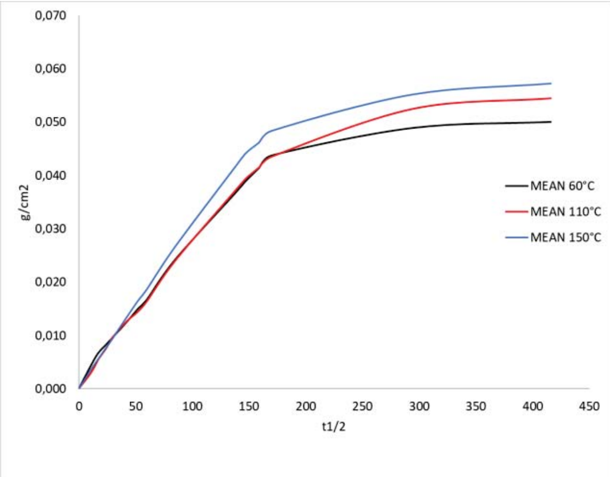

Fig. 1: Water absorption by capillarity curves for sample CA, degraded at 60 °C, 110 °C and 150 °C.

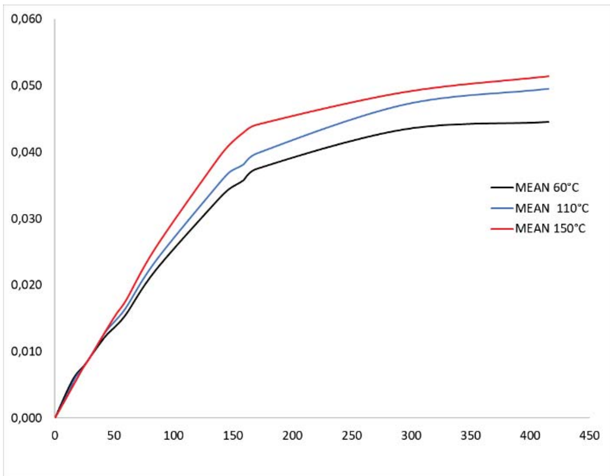

Fig. 2:Water absorption by capillarity curves for sample BA, degraded at 60 °C, 110 °C and 150 °C.

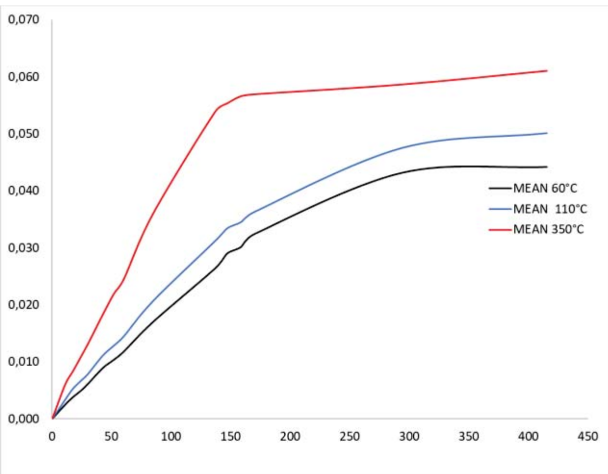

Fig. 3: Water absorption by capillarity curves for sample AA, degraded at 60 °C, 110 °C and 350 °C.

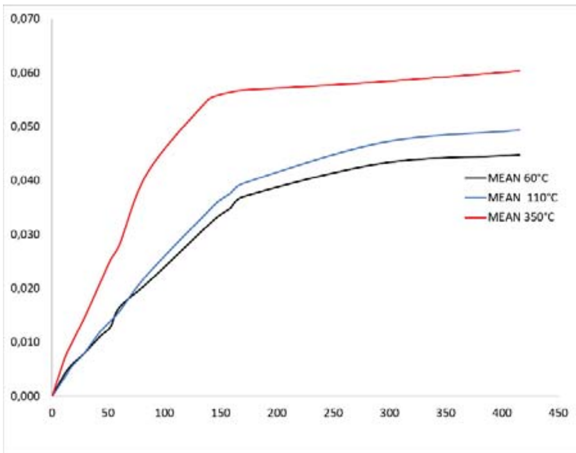

Fig. 4: Water absorption by capillarity curves for sample AB, degraded at 60 °C, 110 °C and 350 °C.

VI. CONCLUSIONS

The carried-out analyses clarify some aspects related to the evaluation of the physical characteristics of the water circulation within a rock, connected with the thermal and mechanical degradation to which the monzogranite can be subjected. In the five studied samples it was found that the verso fracture surface absorbs water less quickly: this is probably due to the presence of greater fractures parallel to the verse compared to the other two, due to microfiltration caused by the cooling of the pluton or to fracturing induced by post intrusion regional tectonic phases.

According to what has been affirmed by Marre [45] in his structural studies on granite plutons, this fracturing should be connected with the late phases of the cooling of the pluton and consequent decrease in the volume of solidifying magma. The monzogranito proved to be a fairly resistant lithotype to the effects of thermal degradation: it should be observed how the values of water absorption and apparent volumes vary very little by heating the sample to 110 °C; the observed volume variations show a standard deviation of the measure corresponding to the precision of the scale used. Analysing the other types of degradation, it is possible to observe an increase in the values of the physical characteristics, and above all in the capillarity coefficient, after heating to 150 °C using the stove, an increase that becomes more sensitive with heating to 350 °C, so it can certainly affirm that, unlike the other degradations, a cycle at 350 °C leads to a variation in the quantity of absorbed water related to a modest increase in the apparent volume, and to the formation of open porosity. It turns out that the thermal cycles produce a degradation of the monzogranite even if it seems difficult to attribute the effects of insolation entirely to the mechanism that leads to an effective disintegration of the granites since it is essential to reach high temperatures to have a significant variation in the physical characteristics of the quantity of water absorbed. However, it seems necessary to hypothesize the intervention of any mechanisms connected with the interaction with water to try to justify further an effective disintegration of the granites.

REFERENCES

[1] M. Franzini, M. Lezzerini, L. Mannella, The stones of medieval buildings in Pisa and Lucca (western Tuscany, Italy). 3 – Green and white-pink quartzites from Mt. Pisano, Eur. J. Mineral., vol. 13, 2001, 187-195.

[2] M. Franzini, M. Lezzerini, F. Marandola, The stones of medieval buildings in Pisa and Lucca (western Tuscany, Italy). 4 – "Agnano breccias" from Mt. Pisano. Eur. J. Mineral., vol. 14, 2002, 447-451.

[3] M. Franzini, M. Lezzerini, The stones of medieval buildings in Pisa and Lucca provinces (western Tuscany, Italy). 1 – The Monte Pisano marble, Eur. J. Mineral., vol. 15, 2003, 217-224.

[4] M. Lezzerini, Mappatura delle pietre presenti nella facciata della chiesa di San Frediano (Pisa, Italia), Atti Soc. Tosc. Sci. Nat., Mem. Serie A, vol. 110, 2005, 43-50.

[5] M. Franzini, M. Lezzerini, F. Origlia, Marbles from the Campiglia Marittima area (Tuscany, Italy), Eur. J. Mineral., vol. 22, 2010, 881-893.

[6] A. Baldanza, A. Gioncada, M. Lezzerini, Historical building stones of the western Tuscany (Italy): the Acquabona Limestones from Mts. Livornesi, Periodico di Mineralogia, vol. 81, 2012, 1-17.

[7] M. Ramacciotti, M. Spampinato, M. Lezzerini, The building stones of the apsidal walls of the Pisa's Cathedral. Atti Soc. Tosc. Sci. Nat., Mem. Serie A, vol. 122, 2015, 55-62.

[8] M. Lezzerini, F. Antonelli, S. Columbu, R. Gadducci, A. Marradi, D. Miriello, L. Parodi, L. Secchiari, A. Lazzeri, Cultural Heritage Documentation and Conservation: Three-Dimensional (3D) Laser Scanning and Geographical Information System (GIS) Techniques for Thematic Mapping of Façade Stonework of St. Nicholas Church (Pisa, Italy), International Journal of Architectural Heritage, vol. 10:1, 2016, 9-19. 10.1080/15583058.2014.924605.

[9] A. Peccerillo, Roman Comagmatic Province (Central Italy): Evidence for subduction related magma genesis, Geology, 13, 1985, 103-106.

[10] A. Peccerillo, On the origin of the Italian Potassic Magmas - Comments. Chem. Geol., vol. 85, 1990, 183-196.

[11] A. Peccerillo, Potassic and ultrapotassic rocks. Compositional characteristics, petrogenesis, and geologic significance, Episodes, 15, 1993, 243-251

[12] A. Peccerillo, S. Conticelli, P. Manetti, Petrological characteristics and the genesis of the recent magmatism of Southern Tuscany and Northern Latium. Period. Mineral., vol. 56, 1987, 157-172.

[13] A. Peccerillo, G. Poli, C. Donati, The Plio-Quaternary magmatism of southern Tuscany and northern Latium: compositional characteristics, genesis, and geodynamic significance, Ofioliti, vol. 26 (2a), 2001, 229-238.

[14] G. Poli, C. Ghezzo, S. Conticelli, Geochemistry of granitic rocks from the Hercynian Sardinia Corsica Batholith: Implication for magma genesis, Lithos, vol. 23, 1989, 247-266.

[15] F. Innocenti, G. Serri, P. Ferrara, P. Manetti, S. Tonarini, Genesis and classification of the rocks of the Tuscan Magmatic Province: thirty years after Marinelli's model. In: "Marinelli Volume", Acta Vulcanologica, vol. 2, 1992, 247-265.

[16] G. Serri, F. Innocenti, P. Manetti, Geochemical and petrological evidence of the subduction of delaminated Adriatic continental lithosphere in the genesis of the Neogene-Quaternary magmatism of Central Italy, Tectonophysics, vol. 223, 1993,117-147.

[17] G. Poli, Genesis and evolution of Miocene-Quaternary intermediate-acidic rocks from the Tuscan Magmatic Province, Per. Mineral., vol. 73, 2004, 187-214.

[18] G. Marinelli, Le intrusioni Terziarie dell'isola d'Elba. Atti Soc. Tosc. Sci. Nat., Mem. Serie A, vol. 68, 1959, 74-116.

[19] F. Saupé, C. Marignac, B. Moine, J. Sonet, J.L. Zimmerman, Datation par les methodes K/Ar et Rb/Sr de quelques roches de la partie orientale de l' Ile d'Elbe (Province de Livourne, Italie), Bull. Mineral., vol. 105, 1982, 236-245.

[20] M. Juteau, Les isotopes radiogéniques et l'évolution de la croûte continentale. C.N.R.S., Centre Rech. Pétrogr. Géochim., Inst. Nat. Polytech. Lorraine, 1984.

[21] G. Ferrara, S. Tonarini, Radiometric geochronology in Tuscany: results and problems, Rend. Soc. It. Mineral. Petrol., vol. 40, 1985, 111-124.

[22] G. Ferrara, S. Tonarini, L' Isola d' Elba: un laboratorio di geocronologia, Mem. Soc. Geol. It., vol. 49, 1993, 227-232.

[23] M. Boccaletti, P. Papini, Ricerche meso e microstrutturali sui corpi ignei neogenici della Toscana. 2: L'intrusione del M. Capanne (Isola d'Elba), Boll. Soc. Geol. It., vol. 108, 1989, 699-710.

[24] C. Maineri, M. Benvenuti, P. Costagliola, A. Dini, P., Lattanzi, G. Ruggieri, I.M. Villa, Sericitic alteration at the La Crocetta deposits (Elba Island, Italy): interplay between magmatism, tectonic and idrotermal activity, Mineralium Deposita, vol. 38, 2003, 67-86.

[25] S. Rocchi, A. Dini, F. Innocenti, S. Tonarini, D.S. Westerman, Elba Island: intrusive magmatism. In: Poli G, Perugini D, Rocchi S, Dini A (eds). Miocene to Recent Plutonism and Volcanism in the Tuscan Magmatic Province (Central Italy), Periodicodi

Mineralogia, vol. 72, 2003, 73-104.
[26] A. Dini, F. Innocenti, S. Rocchi, S. Tonarini, D.S. Westerman, The magmatic evolution of the late Miocene laccolith-pluton-dyke granitic complex of Elba Island, Italy Geological Magazine, vol. 139, 2002, 257-279.
[27] D. Gagnevin, J. Daly, G. Poli, Petrographic, geochemical and isotopic constraints on magma dynamics and mixing in the Miocene Monte Capanne monzogranite (Elba Island, Italy), Lithos, 78, 2004, 157-195.
[28] D. Gagnevin, J. Daly, G. Poli, Morgan D., Microchemical and Sr isotopic investigation of zoned K-feldspar megacrysts: insights into the petrogenesis of a granitic system and disequilibrium crystal growth, Journal of Petrology, vol. 46, 2005, 1689-1724.
[29] D. Gagnevin, J. Daly, G. Poli, Insights into granite petrogenesis from quantitative assessment of the field distribution of enclaves, xenoliths and K-feldspar megacrysts in the Monte Capanne pluton, Italy, Mineralogical Magazine, vol. 72, 2008, 925-940.
[30] D. Gagnevin, J. Daly, A. Kronz, Zircon texture and chemical composition as a guide to magmatic processes and mixing in a granitic environment and coeval volcanic system. Contributions to Mineralogy and Petrology, vol. 159, 2010, 579-596.
[31] D.S. Westerman, A. Dini, F. Innocenti, S. Rocchi, Rise and fall of a nested Christmas-tree laccolith complex, Elba Island, Italy. In: Breitkreu, C, Petford N (eds). Physical geology of high-level magmatic systems, Geol. Soc. London, vol. 234, 2004, 195-213.
[32] F. Farina, A. Dini, F. Innocenti, S. Rocchi, D.S. Westerman, Rapid incremental assembly of the Monte Capanne pluton (Elba Island, Tuscany) by downward stacking of magma sheets, Geological Society of America Bulletin, vol. 122, 2010, 1463-1479.
[33] G. Tedeschi, Il granito dell'elba a Pisa: uso e riuso nel XI e XII secolo. In Niveo de marmore 43-51 Edizione Colombo, Genova, 1992.
[34] M. Franzini, Le pietre Toscane nell'edilizia medioevale della città di Pisa, Mem. Soc. Geol. It., vol. 49, 1992, 233-244.
[35] M. Franzini, L. Leoni, M. Saitta, Revisione di una metodologia analitica per fluorescenza-X, basata sulla correzione completa degli effetti di matrice, Rend. Soc. It. Mineral. Petrog., vol. 31, 1975, 365-378.
[36] M. Lezzerini, M. Tamponi, M. Bertoli, Reproducibility, precision and trueness of X-RAY fluorescence data for mineralogical and/or petrographic purposes", Atti Soc. Tosc. Sci. Nat. Mem. Serie A, vol. 120, 2013, 67-73.
[37] M. Lezzerini, M. Tamponi, M. Bertoli, Calibration of XRF data on silicate rocks using chemicals as in-house standards, Atti Soc. Tosc. Sci. Nat., Mem. Serie A, vol. 121, 2014, 65-70.
[38] EN 1936:2007 – Natural stone test methods - Determination of real density and apparent density, and of total and open porosity.
[39] EN 1925:1999 – Natural stone test methods - Determination of water absorption coefficient by capillarity.
[40] EN 13755:2008 – Natural stone test methods - Determination of water absorption at atmospheric pressure.
[41] M. Franzini, M. Lezzerini, A mercury-displacement method for stone bulk-density determinations, Eur. J. Mineral., vol. 15, 2003, 225-229.
[42] F. Busy, Pétrogenèse des enclaves microgrenues associées aux granitoïdes calco-alcalins: exemple des massifs varisque du Mont Blanc (Alpes occidentales) et miocène du Monte Capanne (Ile d'Elbe, Italie), Pétrographie. Université de Lausanne, 1990.
[43] E.M. Winkler, Stone in architecture. Properties, durability. In: Springer (Ed.), London, 1997.
[44] W.R. Dearman, T.J. Irfan, Assesment of the degree of the weathering in granite using petrographic and physical index tests. In: EPDGI (Ed.), Essais 2.3, International Symposium Unesco-Rilem "Deterioration and protection of stone monuments", Paris, 1978, 1-35.
[45] J. Marre, The structural analysis of granitic rocks. Oxford: North Oxford Academic, 1986.